IEEE Access
Multidisciplinary | Rapid Review | Open Access Journal

Received September 22, 2018, accepted October 6, 2018, date of publication October 11, 2018, date of current version October 31, 2018.

Digital Object Identifier 10.1109/ACCESS.2018.2875344

Underwater Image Restoration Based on A New Underwater Image Formation Model

MOHUA ZHANG[1,2] AND JIANHUA PENG[1]
[1]National Digital Switching System Engineering & Technology Research Center, Zhengzhou 450002, China
[2]College of Computer and Information Engineering, Henan University of Economics and Law, Zhengzhou 450002, China

Corresponding author: Mohua Zhang (mohua.zhang@outlook.com)

This work was supported in part by the Science and Technique Foundation of Henan Province, China, under Grant 152102210087 and in part by the Foundation of Educational Committee of Henan province, China, under Grant 14A520040.

ABSTRACT Underwater image restoration is crucial for compute applications and consumer electronics. However, restoring underwater image from a single image is an odd-ill problem due to the complicated underwater environment. To improve the visual quality of underwater image, we propose an underwater image restoration method. First, we present a new underwater image formation model, which takes the properties of underwater imaging and light into account. Then, a medium transmission estimation method for underwater image based on joint prior is proposed, which, respectively, predicts the medium transmissions of three channels of an underwater image. Moreover, we replace the global background light, which is always used in previous underwater image restoration method, with the colors of light source to correct the color casts appeared on the degraded underwater image. The performance of the proposed method is evaluated on the degraded underwater images taken from different scenes by qualitative and quantitative comparisons. Experimental results demonstrate that our results look more visually pleasing and outperforms the results of several existing methods, especial for the colors and contrast.

INDEX TERMS Underwater image restoration, underwater image enhancement, underwater image prior, underwater imaging.

I. INTRODUCTION

The aim of underwater image restoration and enhancement is to improve the visual quality of images captured under different underwater scenes. In recent years, this research area has attracted increased attention since improving the visibility, contrast, and colors of underwater images is of significance for many computer applications [1], [2]. Nevertheless, enhancing and restoring underwater image from a single image is still challenging due to the complicated underwater environment.

Generally, underwater images are degraded because light is mainly absorbed and scattered by three water constituent particles: micro phytoplankton, colored dissolved organic matter and non-algal particles [3]. When the light propagates in an underwater scenario, the light received by a camera is mainly composed of three kinds of light: direct light, forward scattering light and back scattering light. The received light by a camera suffers from color deviation due to the wavelength dependent light absorption. In general, the red light first disappears with the distance from objects, followed by the orange light, yellow light, purple light, yellow-green light, green light and blue light. This is the main reason why most underwater images are dominated by the bluish or greenish tone. Therefore, to improve the visual quality of underwater image, a method which can remove the effects of back scattering light and wavelength dependent light absorption is needed.

To solve this problem, a variety of methods have been proposed in recent years [6]. Existing methods can be organized into one of four broad categories: single underwater image enhancement method, single underwater image restoration method, deep learning-based method, and additional information method.

Iqbal *et al.* [7] proposed an integrated color model and an unsupervised color correction method to improve the contrast and colors of underwater image. This method is to stretch the dynamic range of the R (red), G (green) and B (blue) channels in RGB color space, and then stretch the dynamic range of the S (saturation) and I (intensity) in HSV color space. Despite the overall contrast being enhanced and color casts being reduced, some regions in the resultant images are under-enhanced and introduce high noise.

2169-3536 © 2018 IEEE. Translations and content mining are permitted for academic research only.
Personal use is also permitted, but republication/redistribution requires IEEE permission.
See http://www.ieee.org/publications_standards/publications/rights/index.html for more information.

Ancuti *et al*. [8] proposed a fusion-based method to enhance the visual quality of underwater images and videos. The method of Ancuti *et al*. fuses a contrast improved underwater image and a color corrected underwater image obtained from input underwater image. In the process of multi-scale fusion, four weights are used to determine which pixel is advantaged to appear in the final image. This method can improve the global contrast and visibility of the degraded underwater image. However, some regions in the resultant images produce over-enhancement or under-enhancement. Ancuti *et al*. [9] proposed a color balance and fusion method for underwater image enhancement, which is a modified version of their method in [8]. Ghani and Isa [10], [11] proposed a Rayleigh-stretched contrast-limited adaptive histogram method to improve the visibility of underwater image, which reduces pixel concentration to constrain the number of under-enhanced and over-enhanced regions. However, this method tends to increase noise and remains some under-enhanced and over-enhanced regions in the resultant images. Zhao *et al*. [12] enhanced underwater images by deriving inherent optical properties. In [13], an underwater image enhancement method based on extended multi-scale retinex was proposed.

Inspired by the observation that the red light usually attenuates faster than the green light and the blue light in an underwater scenario, Carlevaris-Bianca *et al*. [14] proposed a prior that exploits the difference in attenuation among different channels to predict the medium transmission. As a result, the effects of light scattering in an underwater image can be removed. Chiang and Chen [15] combined the dark channel prior dehazing algorithm [16] with the wavelength dependent compensation algorithm to restore underwater image. This method can well restore the underwater images with bluish tone and effectively remove the effects of artificial light. Nevertheless, such a method is limited in processing the underwater images with serious color casts. Galdran *et al*. [17] proposed a Red Channel method, which recovers the lost contrast of underwater image by restoring the colors associated with short wavelengths. Drews, Jr., *et al*. [18] proposed an underwater dark channel prior based on a modification of the dark channel prior [16]. However, underwater dark channel prior does not always hold when there are white objects or artificial light in the underwater scenes. Li *et al*. [19] proposed a systematic method, which includes an underwater image dehazing algorithm and a contrast enhancement algorithm.

With rapid development of deep learning, deep learning-based underwater enhancement methods have emerged in recent years. Li *et al*. [20] proposed a generative adversarial network (GAN) for simulating realistic underwater image from in-air image. Then, based on synthetic underwater images, Li *et al*. designed a Convolutional Neural Network (CNN) structure for underwater image enhancement. This method is effective for the underwater images like the training samples, however it limits in other types of real underwater images. Recently, Li *et al*. [21] proposed a weakly supervised color transfer method to correct the color casts of underwater image based on Cycle-Consistent Adversarial Networks.

Additional information methods mainly include the multiple images captured by polarization filters, stereo images, rough depth of the scene or specialized hardware devices [22]–[26].

Despite these recent efforts, the effectiveness and robustness of the existing methods need to be further addressed. In this paper, we restore the degraded underwater image based on a new underwater image formation model. Unlike previous methods which assume that the atmospheric light is obtained from the brightest region, we assume that the atmospheric light is the same as the colors of the light source. Then, the global background light is estimated via an effective color constancy method. To robustly predict the medium transmission of scene, we joint two underwater image priors by saliency-guided multi-scale fusion technique. Further, the medium transmissions of three color channels (RGB) are achieved based on the optical properties of underwater imaging. Finally, with the estimated global background light and the predicted medium transmissions, the restored underwater image can be obtained according to a new underwater image formation model. Extensively qualitative and quantitative comparisons against several existing methods are performed. Experiments demonstrate that the proposed method not only can restore the degraded underwater image to the relatively genuine colors and natural appearance, but also can increase contrast and visibility. Besides, the proposed method is comparable to and even outperforms several existing methods in terms of the underwater image quality metrics.

This paper introduces the following main contributions:

- Inspired by a new underwater image formation model which takes the fact that wavelength dependent attenuation of underwater light and color casts of underwater image into account, the proposed method solves the problems of low contrast and color casts of the degraded underwater image at the meantime.
- Different from previous methods which obtain the global background light from the brightest region in an input image, we assume the global background light is the same with the colors of light source. In this way, the global background light is easy to be obtained and the color casts of an underwater image can be effective corrected.
- In contrast to previous methods which treat the medium transmissions of the three color channels of an underwater image as the same, we separately predict the medium transmissions of three color channel based on the principle of underwater optical imaging. As a result, the loss of contrast and color casts are better compensated.

The rest of this paper is organized as follows. In section II, we describe the proposed method. In section III, we carry out extensive performance comparisons. In section IV, some discussion and conclusion remarks are given.

II. PROPOSED METHOD

We first introduce a new underwater image formation model. Then, the estimation of the colors of light source is presented. Next, we propose a joint prior, which can be used for the medium transmission prediction. According to the medium transmission of scene and the optical properties of underwater imaging, we predict the medium transmissions of three color channels of an underwater image, respectively. Last, we introduce how to restore the degraded underwater image with the obtained model parameters.

A. A NEW UNDERWATER IMAGE FORMATION MODEL

Most of underwater image restoration methods [14], [18] directly employ the image formation model of outdoor haze [16], [27]–[29]. Such an image formation model can be described as:

$$I^c(x) = J^c(x)t(x) + A^c(1 - t(x)), \quad c \in \{r, g, b\}, \tag{1}$$

where $I(x)$ is the observed image, $J(x)$ is the desired image, A is the global background light and $t(x) = \exp(-\beta d(x)) \in [0,1]$ is the medium transmission which represents the percentage of the scene radiance reaching the camera. β is the attenuation coefficient and d is the depth of scene. However, this model neglects the properties of underwater imaging and lighting conditions, which is not always suitable for underwater scenarios. To comply with the principle of underwater imaging and obtain the better performance, [30] proposed a new underwater image formation model, and can be defined as:

$$I^c(x) = E(x)^c_d + E(x)^c_{bs}, \quad c \in \{r, g, b\}, \tag{2}$$

where $E(x)^c_d$ is the direct light and $E(x)^c_{bs}$ is the back scattering light. Here, following previous methods [14], [16], [18], it also neglects the effects of forward scattering light. The direct light $E(x)^c_d$ is further defined as:

$$E(x)^c_d = J^c(x)t^c(x) = J^c(x)\exp(-\beta^c d(x)), \quad c \in \{r, g, b\}, \tag{3}$$

where $J(x)$ is the underwater image without attenuation (desired image) and $t(x) = \exp(-\beta d(x))$ is the medium transmission. According to the assumption that considering $J(x)$ as a general image taken from a Lambertian Surface, $J(x)$ can be described as the color constancy image formation model [31]:

$$J^c(x) = L^c M^c(x) C^c, \quad c \in \{r, g, b\}, \tag{4}$$

where L is the colors of light source, $M(x)$ is the surface reflectance which represents the restored underwater image without attenuation and color casts, and C is the camera sensitivity parameter. Here, we consider the camera sensitivity parameter C as constant 1. Thus, $J(x)$ can be expressed as:

$$J^c(x) = L^c M^c(x), \quad c \in \{r, g, b\}, \tag{5}$$

According to the Jaffe-McGlamery imaging model [32], [33], the back scattering $E(x)^c_{bs}$ can be defined as:

$$E^c_{bs}(x) = A^c(1 - t^c(x)), \quad c \in \{r, g, b\}, \tag{6}$$

where A is the global background light that may be regarded as the light from infinity when assuming homogeneous lighting along the line of sight. By considering the global background light from infinity B having the same colors with the light source L, the final underwater image formation model can be defined as:

$$I^c(x) = L^c M^c(x)t^c(x) + L^c(1 - t^c(x)), \quad c \in \{r, g, b\}, \tag{7}$$

Known L^c and $t^c(x)$, $M^c(x)$ can be obtained from $I^c(x)$. Therefore, this paper focuses on the estimation of the colors of light source L^c and the medium transmission $t^c(x)$.

B. ESTIMATING THE COLORS OF LIGHT SOURCE

Many methods assume that the global background light can be approximated from the brightest region in the input image. However, the assumption is not available when white objects and artificial light exist in the underwater scenes. To address this problem, we assume underwater image has the homogeneous lighting along the line of sight, and the light from infinity has the same colors with the light source. Then, we regard the global background light in our model as the colors of light source. Inspired by color constancy algorithms which estimate the colors of light source to recover the actual surface colors of an object in a scene, we employ an effective color constancy with local surface reflectance statistics (LSRS) [34] to estimate the colors of light source based on its effectiveness and efficiency. More details can be found in [34]. Other color constancy methods also can be used for the estimation of the colors of light source.

C. JOINTING UNDERWATER IMAGE PRIORS BY SALIENCY-GUIDED MULTI-SCALE FUSION

In recent years, some effective priors, such as dark channel prior [16] and color attenuation prior [38], have been proposed for single image dehazing. Compared with image dehazing research area, there are few works which focus on underwater image priors in the research area of underwater image restoration. Moreover, the existing priors for underwater image show limitations when they are applied to some underwater images captured under different scenes.

Carlevaris-Bianco *et al.* [14] proposed a simple prior for underwater image enhancement by exploiting the difference in attenuation among three color channels in an underwater image. Here, we call it intensity attenuation difference prior (IATP). Based on IATP, the medium transmission of an underwater scene can be estimated. First, IATP is defined as comparing the maximum intensity of the red channel to the maximum intensity of the green and blue channels over an image patch, and is expressed as:

$$D(x) = \max_{x\in\Omega, c\in r}(I^c(x)) - \max_{x\in\Omega, \; c\in\{g,b\}}(I^c(x)), \tag{8}$$

where $D(x)$ is the IATP, $I^c(x)$ is the input image and Ω is the size of an image patch. According to IATP, the medium transmission of an underwater image $t(x)$ can be estimated

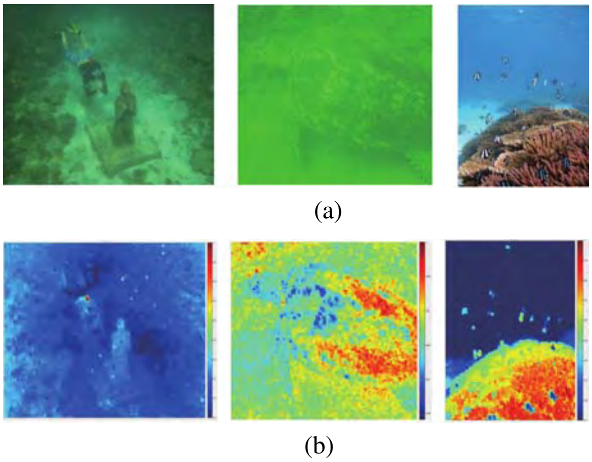

FIGURE 1. **Several examples of the inaccurate estimation of IATP. (a) Several underwater images. (b) Medium transmissions estimated by IATP. In the colorized medium transmissions, reddish colors represent the pixels have higher values (*i.e.*, these pixels are close to the camera) and bluish colors represent the pixels have lower values (*i.e.*, these pixels are far away from the camera).**

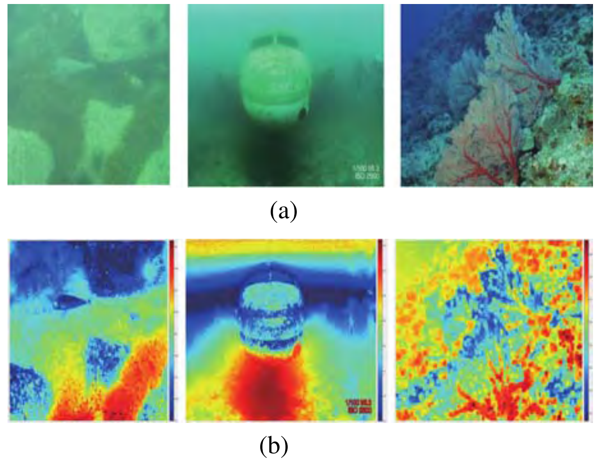

FIGURE 2. **Several examples of the inaccurate estimation of UDCP. (a) Several underwater images. (b) Medium transmission estimated by UDCP. In the colorized medium transmissions, reddish colors represent the pixels have higher values and bluish colors represent the pixels have lower values.**

by:

$$t(x) = D(x) + (1 - \max_{x} D(x)), \tag{9}$$

Although IATP is relatively effective for many underwater scenes, it produces inaccurate estimation in some regions of the medium transmission for some underwater images captured under challenging scenes. Fig. 1 shows several inaccurate results of the medium transmission estimated by IATP.

Drew, Jr., *et al.* [18] proposed an underwater dark channel prior (UDCP) based on a modification of the traditional dark channel prior (DCP) which is very effective for the outdoor haze image. DCP is proposed based on statistics of experiments on haze-free images, which represents most local patches in haze-free images contain some pixels which have very low intensities in at least one color channel. However, Drew *et al.* found that the DCP is not available for many practical underwater scenes since red channel is serious attenuated (approximate zero). This fact makes the information of red channel unreliable for DCP. Thus, Drew *et al.* proposed an UDCP which just considers the information provided by the green and blue channels. UDCP represents that most local patches in haze-free underwater images contain some pixels which have very low intensities in at least one color channel between the green channel and the blue channel. The medium transmission $t(x)$ based on UDCP can be estimated by:

$$t(x) = 1 - \min_{c}(\min_{x \in \Omega}(\frac{I^c}{B^c})), \quad c \in \{g, b\}, \tag{10}$$

where I^c is the input image, B^c is the global background light, and Ω denotes the size of an image patch. UDCP also produces inaccurate estimation in some regions of the medium transmission. Fig. 2 shows several inaccurate results of the medium transmission estimated by UDCP.

We found that the use of a single prior is relatively effective but insufficient. To improve the robustness of the proposed framework, we attempt to joint the above-mentioned IATP and UDCP for medium transmission estimation. The main idea behind the use of the joint prior is that we experientially found the salient regions of the medium transmission estimated by IATP or UDCP are relatively accurate. However, it is hard to prove this findings mathematically. We leave this work in the future. Besides, both IATP and UDCP assume that the red light disappear firstly. Similar assumption can accelerate the fusion of these priors. In fact, we can directly use other effective and accurate underwater image restoration prior; however, there is no accurate and robust enough prior available for challenging scenes. To our best knowledge, the IATP and UDCP are relatively most effective priors. To joint these two priors, a saliency-guided multi-scale fusion scheme driven by the intrinsic properties of input medium transmission is employed, which highlights the salient regions in the restored results. In other word, the salient regions in the restored results are relatively accurate. Compared with other joint schemes such as single scale fusion and choosing the maximum between inputs, the multi-scale fusion scheme can reduce the introduction of undesirable halos and noise [8]. Therefore, we use the saliency of input medium transmissions to determine which pixel is advantaged to appear in the final medium transmission. The final medium transmission $t_f(x)$ can be obtained by summing the fused contribution of all inputs, and can be expressed as:

$$t_f^l(x) = \sum_{k=1}^{K} G^l\{\bar{S}^k(x)\} L^l\{t^k(x)\}, \tag{11}$$

where $t_f^l(x)$ is the final medium transmission, $l = 5$ is the number of the pyramid levels, $K = 2$ is the number of the input, $G\{\bar{S}(x)\}$ is the Gaussian pyramid operation which decomposes the normalized saliency weight map $\bar{S}(x)$ and $L\{t(x)\}$ is the Laplacian pyramid operation [39] which decomposes the input medium transmission $t(x)$ (*i.e.*,

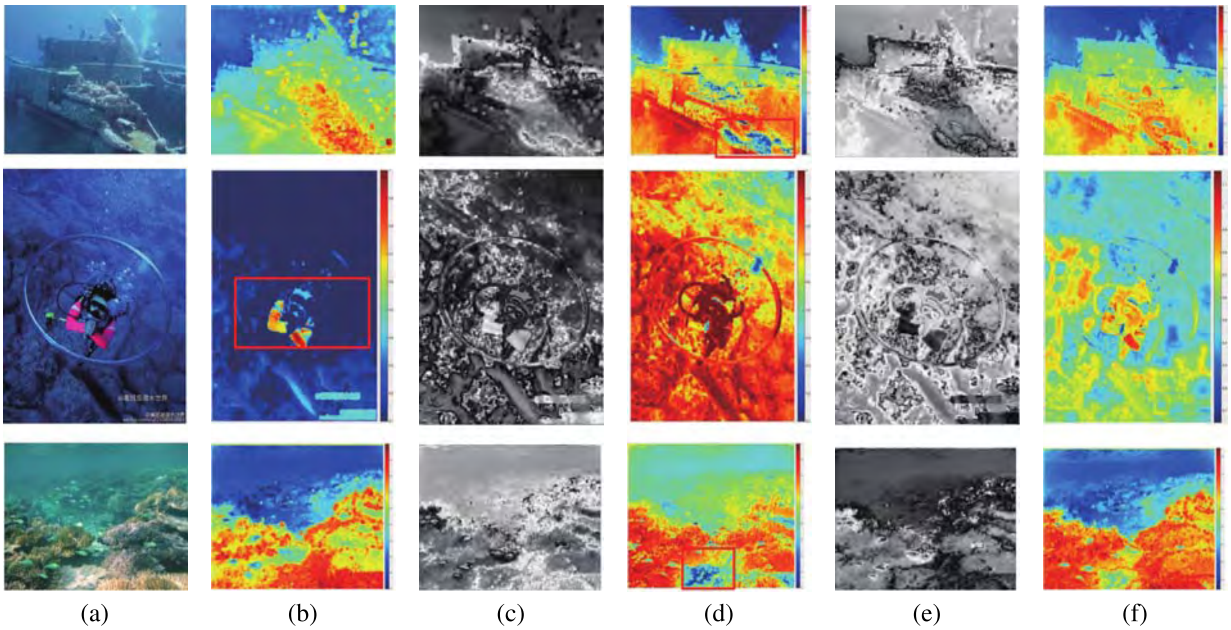

FIGURE 3. Some results of our saliency-guided multi-scale fusion scheme. (a) Raw underwater images. (b) Medium transmissions estimated by IATP. (c) Normalized saliency weight maps of (b). (d) Medium transmissions estimated by UDCP. (e) Normalized saliency weight maps of (d). (f) Fused medium transmissions by our scheme. Red boxes represent the inaccurate estimation.

the medium transmission estimated by IATP $t_{LAT}(x)$ and the medium transmission estimated by UDCP $t_{UDCP}(x)$). In our fusion scheme, we employ a frequency-tuned salient region detection algorithm since it is computationally efficient [40]. Firstly, the saliency weight map of input medium transmission is calculated. Then, to yield consistent results, the obtained saliency weight map is normalized, and can be computed as:

$$\bar{S}^k(x) = \frac{S^k(x)}{\sum_{k=1}^{K} S^k(x)}, \tag{12}$$

where $\bar{S}(x)$ is the normalized saliency weight map, $S(x)$ is the obtained saliency weight map, and $K = 2$ is the number of the input. In recent years, there have emerged many the state-of-the-art salient region detection algorithms [41], [42]. Some of these algorithms also may be available in our method. In Fig. 3, we present some results of our saliency-guided multi-scale fusion scheme.

As shown is Fig. 3, the fused medium transmissions are relatively more accurate when compared with the inaccurate estimation presented on the Fig. 3(b) and Fig. 3(d). For example, the regions of red box in Fig. 3(b) and Fig. 3(d) are corrected in the final medium transmissions by saliency-guided multi-scale fusion scheme where saliency weight map determines which pixel is advantaged to appear in the final fusion result. Because the IATP and UDCP are calculated block-by-block, we incorporate the guided filter [43] to refine the final medium transmission to reduce the blocking artifacts.

D. ESTIMATING THE MEDIUM TRANSMISSIONS OF THREE COLOR CHANNELS

In most of underwater image restoration methods, the authors assume that three color channels of an underwater image have the identical medium transmission. However, different channels of an underwater image should have different medium transmissions due to the different attenuation coefficient β. In the new underwater image formation model, the medium transmission is defined as:

$$t^c(x) = \exp(-\beta^c d(x)), \quad c \in \{r, g, b\}, \tag{13}$$

According to [15] and [44], Eq. (13) can be rewritten as:

$$t^c(x) = (Nrer^c)^{d(x)}, \quad c \in \{r, g, b\}, \tag{14}$$

where $Nrer^c$ represents the normalized residual energy ratio. In general water [15], [45], $Nrer^c$ can be further expressed as:

$$Nrer^c = \begin{cases} 0.8 \sim 0.85 & c = r \\ 0.93 \sim 0.97 & c = g \\ 0.95 \sim 0.99 & c = b \end{cases} \tag{15}$$

If one knows the depth of scene $d(x)$, the medium transmissions of three color channels can be estimated using Eq. (14) and Eq. (15). Before, we have obtained the refined medium transmission estimated by joint prior. So, the depth of scene $d(x)$ can be calculated as:

$$d(x) = \frac{log(t_r(x))}{log(Nrer)}, \tag{16}$$

where $t_r(x)$ is the refined medium transmission and $Nrer$ is the normalized residual energy ratio. Thus, the medium

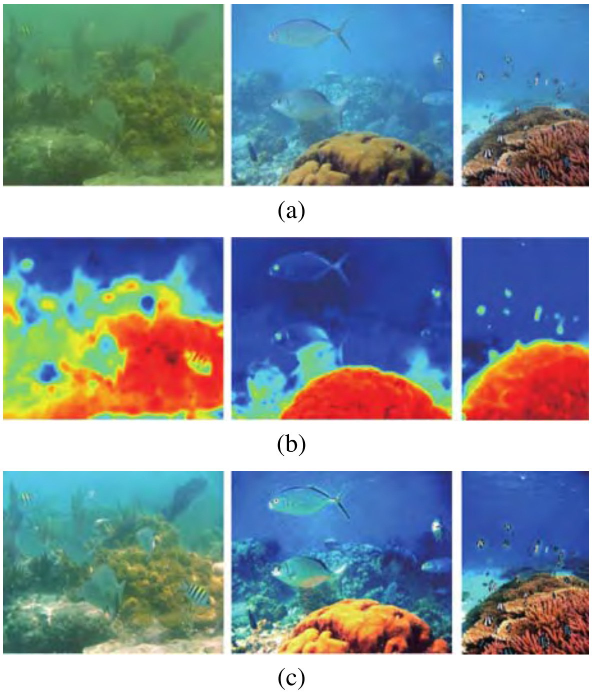

FIGURE 4. Restored results with our method. (a) Raw underwater images. (b) Refined medium transmissions estimated by the proposed joint prior. (c) Restored results by our method.

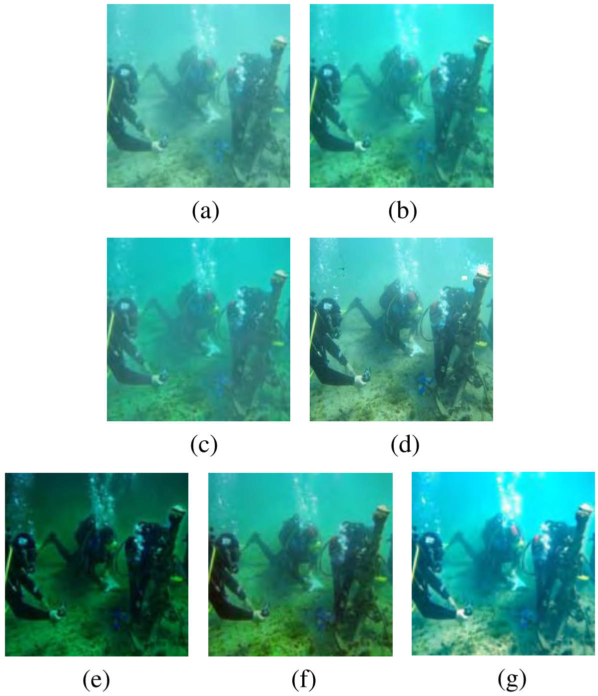

FIGURE 5. Qualitative comparison on image "divers". (a) Raw underwater image with size of 1000 × 700. (b) Result of DCP [16]. (c) Result of CAP [38]. (d) Result of IATP [14]. (e) Result of UDCP [18]. (f) Result of ODM [19]. (g) Our result.

transmissions of three color channels $t^c(x)$ can be estimated as:

$$t^c(x) = (Nrer^c)^{\frac{log(t_r(x))}{log(Nrer)}}, \quad c \in \{r, g, b\}, \tag{17}$$

E. RESTORING UNDERWATER IMAGE

According to the new underwater image formation model, the restored underwater image $M^c(x)$ can be obtained by:

$$M^c(x) = \frac{I^c(x) - L^c + L^c t^c(x)}{\max(\tau^c, L^c t^c(x))}, \quad c \in \{r, g, b\}. \tag{18}$$

where $I^c(x)$ is the input underwater image, L^c is the colors of light source, $t^c(x)$ is the medium transmission, τ^c is the parameter which avoids introducing noise. Fig. 4 shows some restored results with our method.

In Fig. 4, we just show the refined medium transmissions obtained from joint prior because it is hard to distinguish the medium transmissions of three color channels in color image form. As shown in Fig. 4, the refined medium transmissions indicate that our method can estimate the medium transmission (depth) of scene in a relatively accurate manner. Moreover, our restored results are characterized by natural colors and increased visibility.

III. EXPERIMENTS

We collect several raw underwater images which are often used in the comparison experiments. With these images, we evaluate the performance of our proposed method and compare with several existing methods. In our method, the size of image patch Ω is set to 9 × 9, the patch size of guided filter is 7 × 7 and the constraint parameter τ^c is set to 0.3, 0.2, and 0.2 for red, green, and blue channels, respectively. $Nrer$, $Nrer^r$, $Nrer^g$, and $Nrer^b$ are set to 0.8, 0.85, 0.97, and 0.99, respectively.

The compared methods include single image dehazing methods (*i.e.*, DCP [16] and CAP [38]) and single underwater image restoration methods (*i.e.*, IATP [14], UDCP [18] and ODM [19]). DCP method is a classical single image dehazing method. CAP method is the state-of-the-art image dehazing method which is based on color attenuation prior for outdoor hazy image. Our method is compared with DCP and CAP methods in order to show that our method is more suitable for underwater scene than the outdoor image dehazing methods. IATP and UDCP methods are based on single underwater image prior. The main purpose of comparing our method with IATP and UDCP methods is to demonstrate that our joint prior is more effective than single IATP or UDCP. ODM method is an underwater image restoration method based on minimum information loss. We compare our method with ODM method to demonstrate the effectiveness and robustness of our method for underwater images.

A. QUALITATIVE COMPARISON

In Figs. 5-9, we present the qualitative comparisons. Observing the qualitative comparison results, DCP and CAP methods have few effects on the raw underwater images because the priors obtained from outdoor hazy images are not suitable for underwater scenes. IATP method can improve the visual quality of images "rock" and "coral", but it shows limitations when it is used to process the underwater images

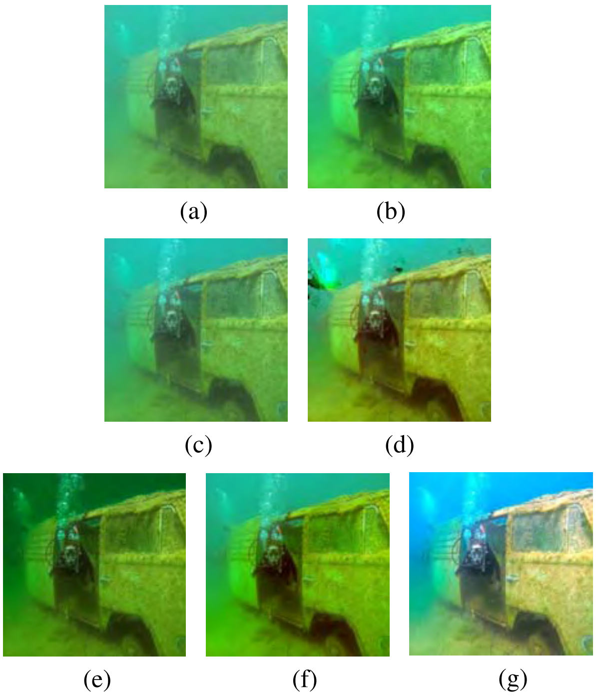

FIGURE 6. **Qualitative comparison on image "bus". (a) Raw underwater image with size of 1000 × 700. (b) Result of DCP [16]. (c) Result of CAP [38]. (d) Result of IATP [14]. (e) Result of UDCP [18]. (f) Result of ODM [19]. (g) Our result.**

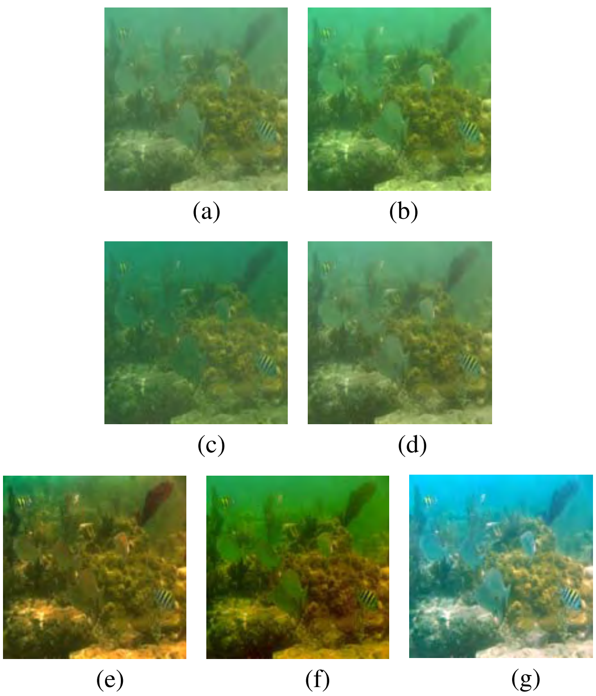

FIGURE 7. **Qualitative comparison on image "fish". (a) Raw underwater image with size of 1000 × 700. (b) Result of DCP [16]. (c) Result of CAP [38]. (d) Result of IATP [14]. (e) Result of UDCP [18]. (f) Result of ODM [19]. (g) Our result.**

with greenish tone and low contrast, such as images "divers" and "fish". The poor robustness of IATP method potentially reduces its practical applications. For UDCP method,

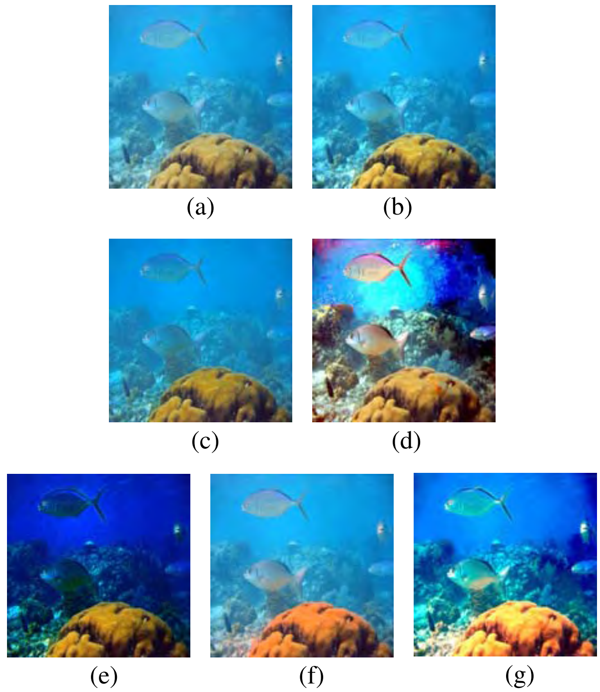

FIGURE 8. **Qualitative comparison on image "rock". (a) Raw underwater image with size of 1000 × 700. (b) Result of DCP [16]. (c) Result of CAP [38]. (d) Result of IATP [14]. (e) Result of UDCP [18]. (f) Result of ODM [19]. (g) Our result.**

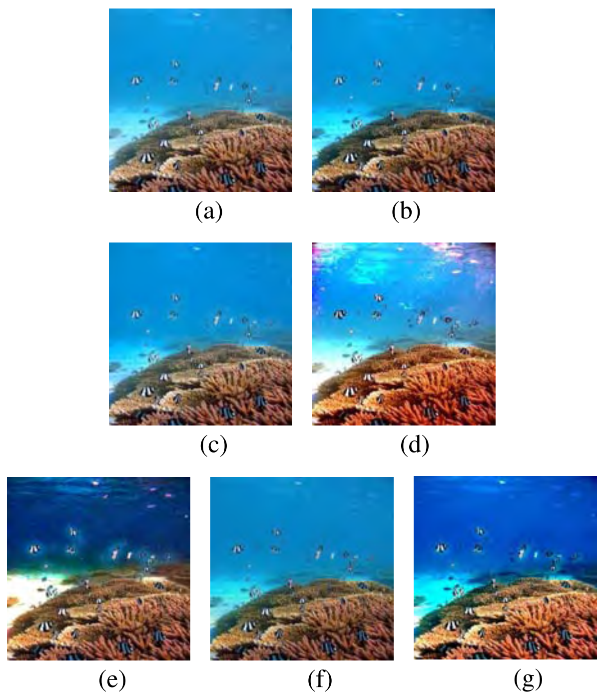

FIGURE 9. **Qualitative comparison on image "coral". (a) Raw underwater image with size of 1000 × 700. (b) Result of DCP [16]. (c) Result of CAP [38]. (d) Result of IATP [14]. (e) Result of UDCP [18]. (f) Result of ODM [19]. (g) Our result.**

it introduces over-compensated regions, such as the background regions in images "rock" and "coral" because of the over-estimation of the medium transmission. ODM method can effectively remove the effects of haze in the underwater

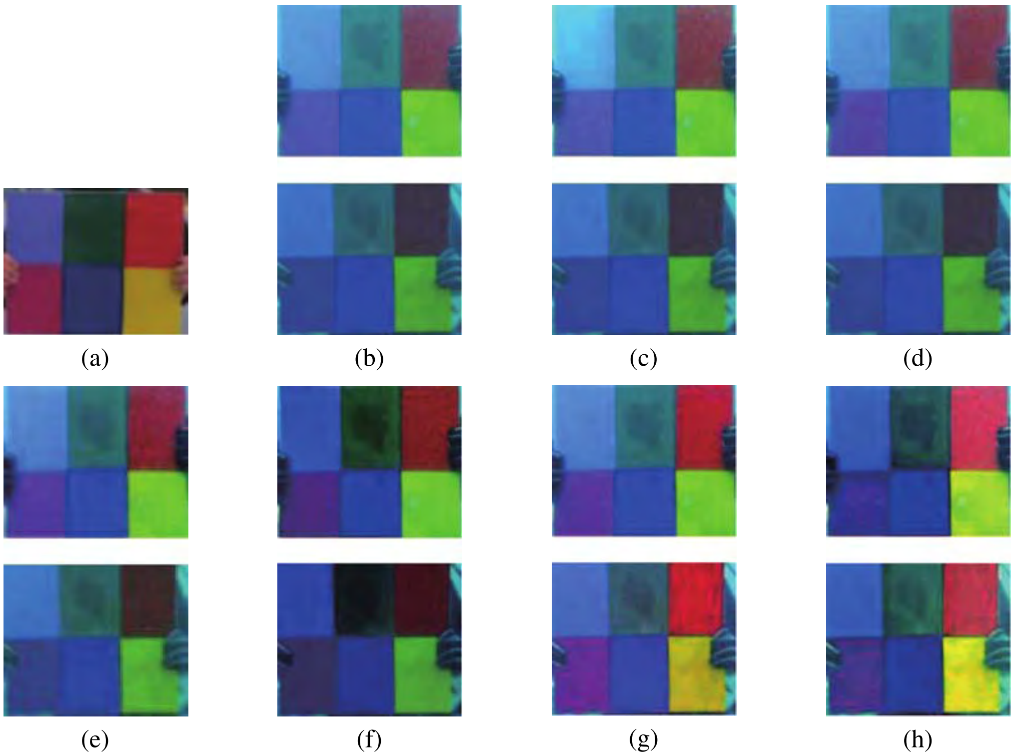

FIGURE 10. Color accuracy comparisons. (a) Color-checker image with six color taken in the air. (b) Color-checker images taken at the depth of 5 meters (top) and 10 meters (bottom). (c) Results of DCP [16]. (d) Results of CAP [38]. (e) Results of IATP [14]. (f) Results of UDCP [18]. (g) Results of ODM [19]. (h) Our results.

images. Moreover, the results of ODM method look natural. However, few details and colors of raw underwater images are veiled by ODM method. Observing our results, they retain vivid colors of the scenes and show the improved contrast and brightness based on the accurate estimation of the medium transmissions and the colors of light source. Compared with the results of other methods, our results with few color casts are more visually pleasing. To further compare the color correction performance of different methods, we present the compared results on two underwater color-checker images in Fig. 10.

As shown in Fig. 10(b), compared with color-checker image taken in the air, some colors decay due to the wavelength dependent light attenuation and back scattering light. As for Fig. 10(c)-(f), DCP, CAP, IATP, and UDCP methods can not well restore the colors of underwater color-checker images. As for Fig. 10(g)-(h), ODM and our methods change the colors of underwater color-checker images because the image formation models in this two methods take the selective attenuation of underwater light into consideration. In contrast to the results of ODM method, the colors of our results subjectively look more close to those of the color-checker image taken in the air.

B. QUANTITATIVE COMPARISON

To quantitatively compare the results of the above-mentioned methods, we apply underwater color image quality evaluation (UCIQE) [46] to assess the visual quality of the results in Figs. 5-9. In addition, the patch-based contrast quality index (PCQI) [47] is applied to evaluate the contrast variations.

UCIQE is defined as a linear combination of chroma, saturation and contrast:

$$UCIQE = c_1 \times \sigma_c + c_2 \times con_l + c_3 \times \mu_s. \tag{19}$$

where σ_c is the standard deviation of chroma, con_l denotes the contrast of luminance, μ_s represents the average of saturation, and c_1, c_2, c_3 are weighted coefficients. Here, we follow the recommended weighted coefficients (*i.e.*, $c_1 = 0.4680$, $c_2 = 0.2745$, $c_3 = 0.2576$). The higher UCIQE values indicate the image has better visual quality.

PCQI is to predict the human perception of contrast variations, which can be expressed as:

$$PCQI = \frac{1}{M}\sum_{i=1}^{M} q_i(x_i, y_i)q_c(x_i, y_i)q_s(x_i, y_i). \tag{20}$$

where M represents the total number of the patches in the image, q_i, q_c and q_s are three comparison functions. The higher PCQI values denotes that the image has better contrast. Table 1 shows the comparative values in terms of the UCIQE and PCQI. The values in bold represent the best results.

The quantitative results summarized in Table 1 show that our method outperforms the compared methods in terms of the average values of UCIQE and PCQI. The highest average values of UCIQE and PCQI indicate that our method has better visual quality and contrast improvement when compared

TABLE 1. Quantitative results in terms of UCIQE and PCQI.

Metric	Method	diver	bus	fish	rock	coral	Average
UCIQE	DCP [16]	0.4794	0.5606	0.4734	0.6108	0.6983	0.5645
	CAP [38]	0.4384	0.5153	0.4318	0.5592	0.6842	0.5258
	IATP [14]	0.5044	0.6290	0.4458	**0.6967**	**0.7575**	0.6074
	UDCP [18]	0.5211	0.5194	0.5449	0.6010	0.7224	0.5817
	ODM [19]	**0.5702**	0.6025	0.5327	0.6090	0.6784	0.5986
	Ours	0.5326	**0.6424**	**0.5658**	0.6856	0.7325	**0.6316**
PCQI	DCP [16]	0.8012	1.0533	0.9937	1.0147	0.8299	0.9385
	CAP [38]	0.6840	0.9588	0.7696	0.8307	0.8077	0.8101
	IATP [14]	0.4612	0.7662	0.7468	0.8951	0.6658	0.7070
	UDCP [18]	0.7164	0.9030	1.0494	0.7756	**0.9794**	0.8848
	ODM [19]	0.7730	1.0122	1.0032	0.9869	0.7997	0.9150
	Ours	**0.8594**	**1.1065**	**1.1268**	**1.0212**	0.9080	**1.0043**

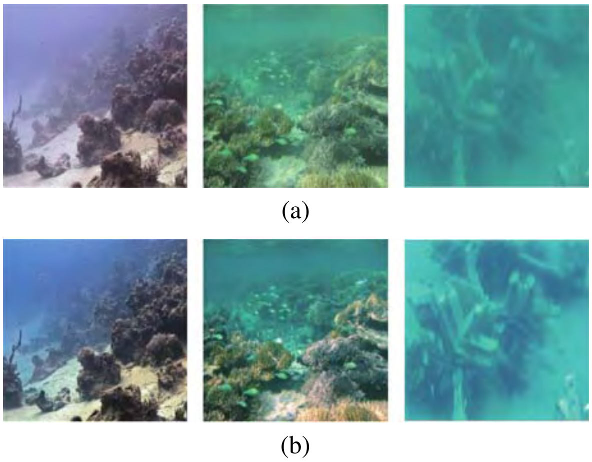

(a) (b)

FIGURE 11. Our results. (a) Raw underwater images. (b) Restored results by our method.

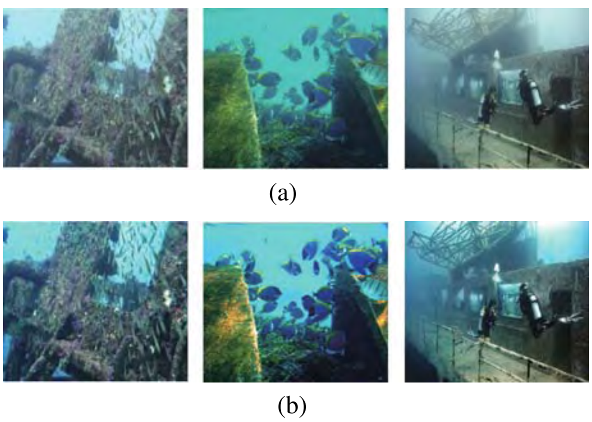

(a) (b)

FIGURE 12. Our results. (a) Raw underwater images. (b) Restored results by our method.

to other methods. The result of UDCP for image ''coral'' ranks first best in terms of PCQI, but there are obvious artifacts in the background. The highest score for image ''coral'' may be from the magnified artifacts. As can be seen in images ''rock'' and ''coral'', there are artifacts and color casts in the background regions of the results of IATP, but these two images rank first best in terms of UCIQE. Obviously, our results without artifacts and color casts look more visually pleasing. More restored results by our method can be seen in Figs. 11 and 12.

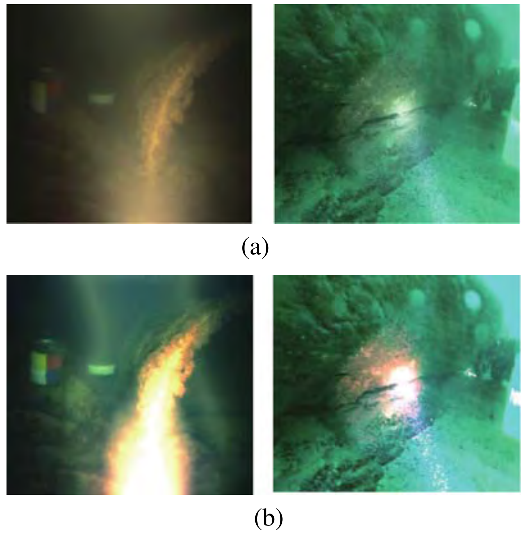

(a) (b)

FIGURE 13. Failure cases. (a) Raw underwater images with non-uniformly lighting. (b) Restored results by our method.

IV. CONCLUSION AND FUTURE WORK

In this paper, we have presented an underwater image restoration method based on joint prior using a new underwater image formation model. By jointing underwater image priors and considering the optical properties of underwater imaging, the medium transmissions of three color channels of an underwater image are estimated, respectively. In this way, the estimated medium transmissions are more accurate and robust than those of traditional methods, which leads to the improved contrast and brightness of our restored results. Based on the assumption that the global background light is the same with the colors of light source, the color casts of underwater image can be effectively removed based on a new underwater image formation model. Experimental results demonstrate the advantage of the proposed method when compared with several existing methods.

However, the proposed method also shows some limitations when it is used to restore the underwater images with non-uniformly lighting. Fig. 13 shows two failure cases of our method. In Fig. 13, the visibility and contrast are improved by our method. Meanwhile, the non-uniformly lighting is magnified, which results in poor visual quality of the restored results. For future work, we plan to add a non-uniformly lighting detection and removal algorithm in our method.

ACKNOWLEDGMENT

The authors sincerely thank the editors and anonymous reviewers for their valuable comments.

REFERENCES

[1] G. L. Foresti, "Visual inspection of sea bottom structures by an autonomous underwater vehicle," *IEEE Trans. Syst., Man, Cybern. B. Cybern.*, vol. 31, no. 5, pp. 691–705, Oct. 2001.

[2] N. J. C. Strachan, "Recognition of fish species by colour and shape," *Image Vis. Comput.*, vol. 11, no. 4, pp. 2–10, 1993.

[3] C. D. Mobley, *Light and Water: Radiative Transfer in Natural Waters*. New York, NY, USA: Academic, 1994.

[4] A. Yamashita, M. Fujii, and T. Kaneko, "Color registration of underwater images for underwater sensing with consideration of light attenuation," in *Proc. IEEE Int. Conf. Robot. Automat.*, Apr. 2007, pp. 4570–4575.

[5] Z. Zhang and D. Tao, "Slow feature analysis for human action recognition," *IEEE Trans. Pattern Anal. Mach. Intell.*, vol. 34, no. 3, pp. 436–450, Mar. 2012.

[6] R. Schettini and S. Corchs, "Underwater image processing: State of the art of restoration and image enhancement methods," *EURASIP J. Adv. Signal Process.*, vol. 2010, no. 14, p. 746052, Dec. 2010.

[7] K. Iqbal, M. Odetayo, A. James, R. A. Salam, and A. Z. Hj Talib, "Enhancing the low quality images using unsupervised colour correction method," in *Proc. IEEE Int. Conf. Syst., Man Cybern.*, Oct. 2010, pp. 1703–1709.

[8] C. Ancuti, C. O. Ancuti, T. Haber, and P. Bekaert, "Enhancing underwater images and videos by fusion," in *Proc. IEEE Conf. Comput. Vis. Pattern Recognit.*, Jun. 2012, pp. 81–88.

[9] C. O. Ancuti, C. Ancuti, C. De Vleeschouwer, and P. Bekaert, "Color balance and fusion for underwater image enhancement," *IEEE Trans. Image Process.*, vol. 27, no. 1, pp. 379–393, Jan. 2018.

[10] A. S. A. Ghani and N. A. M. Isa, "Underwater image quality enhancement through integrated color model with Rayleigh distribution," *Appl. Soft Comput.*, vol. 27, pp. 219–230, Feb. 2015.

[11] A. S. A. Ghani and N. A. M. Isa, "Enhancement of low quality underwater image through integrated global and local contrast correction," *Appl. Soft Comput.*, vol. 37, pp. 332–344, Dec. 2015.

[12] X. Zhao, T. Jin, and S. Qu, "Deriving inherent optical properties from background color and underwater image enhancement," *Ocean Eng.*, vol. 94, pp. 163–172, Jan. 2015.

[13] S. Zhang, T. Wang, J. Dong, and H. Yu, "Underwater image enhancement via extended multi-scale Retinex," *Neurocomputing*, vol. 245, pp. 1–9, Jul. 2017.

[14] N. Carlevaris-Bianco, A. Mohan, and R. M. Eustice, "Initial results in underwater single image dehazing," in *Proc. IEEE Conf. OCEANS*, Sep. 2010, pp. 1–8.

[15] J. Y. Chiang and Y.-C. Chen, "Underwater image enhancement by wavelength compensation and dehazing," *IEEE Trans. Image Process.*, vol. 21, no. 4, pp. 1756–1769, Apr. 2012.

[16] K. He, J. Sun, and X. Tang, "Single image haze removal using dark channel prior," *IEEE Trans. Pattern Anal. Mach. Intell.*, vol. 33, no. 12, pp. 2341–2353, Dec. 2011.

[17] A. Galdran, D. Pardo, A. Picón, and A. Alvarez-Gila, "Automatic red-channel underwater image restoration," *J. Vis. Commun. Image Represent.*, vol. 26, pp. 132–145, Jan. 2015.

[18] P. L. J. Drews, Jr., E. R. Nascimento, S. S. C. Botelho, and M. F. M. Campos, "Underwater depth estimation and image restoration based on single images," *IEEE Comput. Graph. Appl.*, vol. 36, no. 2, pp. 24–35, Mar./Apr. 2016.

[19] C.-Y. Li, J.-C. Guo, R.-M. Cong, Y.-W. Pang, and B. Wang, "Underwater image enhancement by dehazing with minimum information loss and histogram distribution prior," *IEEE Trans. Image Process.*, vol. 25, no. 12, pp. 5664–5677, Dec. 2016.

[20] J. Li, K. A. Skinner, R. M. Eustice, and M. Johnson-Roberson, "WaterGAN: Unsupervised generative network to enable real-time color correction of monocular underwater images," *IEEE Robot. Automat. Lett.*, vol. 3, no. 1, pp. 387–394, Jan. 2018.

[21] C. Li, J. Guo, and C. Guo, "Emerging from water: Underwater image color correction based on weakly supervised color transfer," *IEEE Signal Process. Lett.*, vol. 25, no. 3, pp. 323–327, Mar. 2018.

[22] D.-M. He and G. G. L. Seet, "Divergent-beam Lidar imaging in turbid water," *Opt. Lasers Eng.*, vol. 41, no. 1, pp. 217–231, 2004.

[23] Y. Y. Schechner and N. Karpel, "Clear underwater vision," in *Proc. IEEE Int. Conf. Comput. Vis. Pattern Recognit.*, Jul./Jun. 2004, p. 1.

[24] Y. Y. Schechner and N. Karpel, "Recovery of underwater visibility and structure by polarization analysis," *IEEE J. Ocean. Eng.*, vol. 30, no. 3, pp. 570–587, Jul. 2005.

[25] T. Treibitz and Y. Y. Schechner, "Active polarization descattering," *IEEE Trans. Pattern Anal. Mach. Intell.*, vol. 31, no. 3, pp. 385–399, Mar. 2009.

[26] M. Sheinin and Y. Y. Schechner, "The next best underwater view," in *Proc. IEEE Conf. Comput. Vis. Pattern Recognit.*, Jun. 2016, pp. 3764–3773.

[27] S. G. Narasimhan and S. K. Nayar, "Chromatic framework for vision in bad weather," in *Proc. IEEE Conf. Comput. Vis. Pattern Recognit.*, Jun. 2000, pp. 598–605.

[28] R. T. Tan, "Visibility in bad weather from a single image," in *Proc. IEEE Int. Conf. Comput. Vis. Pattern Recognit.*, Jun. 2008, pp. 1–8.

[29] D. Berman, T. Treibitz, and S. Avidan, "Non-local image dehazing," in *Proc. IEEE Int. Conf. Comput. Vis. Pattern Recognit.*, Jun. 2016, pp. 1674–1682.

[30] F. Codevilla *et al.* (2016). "General participative media single image restoration." [Online]. Available: https://arxiv.org/abs/1603.01864v1

[31] J. van de Weijer, T. Gevers, and A. Gijsenij, "Edge-based color constancy," *IEEE Trans. Image Process.*, vol. 16, no. 9, pp. 2207–2214, Sep. 2007.

[32] J. S. Jaffe, "Computer modeling and the design of optimal underwater imaging systems," *IEEE J. Ocean. Eng.*, vol. 15, no. 2, pp. 101–111, Apr. 1990.

[33] B. McGlamery, "A computer model for underwater camera systems," *Proc. SPIE*, vol. 0208, pp. 221–231, Mar. 1980.

[34] S. Gao *et al.*, "Efficient color constancy with local surface reflectance statistics," in *Proc. Eur. Conf. Comput. Vis.*, 2014, pp. 158–173.

[35] G. Buchsbaum, "A spatial processor model for object colour perception," *J. Franklin Inst.*, vol. 310, no. 1, pp. 1–26, Jul. 1980.

[36] E. H. Land and J. J. McCann, "Lightness and Retinex theory," *J. Opt. Soc. Amer.*, vol. 61, no. 1, pp. 1–11, 1971.

[37] A. Chakrabarti, K. Hirakawa, and T. Zickler, "Color constancy with spatio-spectral statistics," *IEEE Trans. Pattern Anal. Mach. Intell.*, vol. 34, no. 8, pp. 1509–1519, Aug. 2012.

[38] Q. Zhu, J. Mai, and L. Shao, "A fast single image haze removal algorithm using color attenuation prior," *IEEE Trans. Image Process.*, vol. 24, no. 11, pp. 3522–3533, Nov. 2015.

[39] P. Burt and T. Adelson, "The Laplacian pyramid as a compact image code," *IEEE Trans. Image Commun.*, vol. 31, no. 4, pp. 532–540, Apr. 1983.

[40] R. Achanta, S. Hemami, F. Estrada, S. Susstrunk, "Frequency-tuned salient region detection," in *Proc. IEEE Int. Conf. Comput. Vis. Pattern Recognit.*, Jun. 2009, pp. 1597–1604.

[41] M.-M. Cheng, N. J. Mitra, X. Huang, P. H. S. Torr, and S.-M. Hu, "Global contrast based salient region detection," in *Proc. IEEE Int. Conf. Comput. Vis. Pattern Recognit.*, Jun. 2011, pp. 569–582.

[42] J. Kim, D. Han, Y.-W. Tai, and J. Kim, "Salient region detection via high-dimensional color transform and local spatial support," *IEEE Trans. Image Process.*, vol. 25, no. 1, pp. 9–23, Jan. 2016.

[43] K. He, J. Sun, and X. Tang, "Guided image filtering," in *Proc. Eur. Conf. Comput. Vis.*, 2010, pp. 1–14.

[44] S. Q. Duntley, "Light in the sea," *J. Opt. Soc. Amer.*, vol. 53, no. 2, pp. 214–233, 1963.

[45] N. Jerlov, *Optical Oceanography*. Amsterdam, The Netherlands: Elsevier, 1968.

[46] M. Yang and A. Sowmya, "An underwater color image quality evaluation metric," *IEEE Trans. Image Process.*, vol. 24, no. 12, pp. 6062–6071, Dec. 2015.

[47] S. Wang, K. Ma, H. Yeganeh, Z. Wang, and W. Lin, "A patch-structure representation method for quality assessment of contrast changed images," *IEEE Signal Process. Lett.*, vol. 22, no. 12, pp. 2387–2390, Dec. 2015.

MOHUA ZHANG received the M.S. degree in computer science from Northwestern Polytechnical University, China, in 2006. He is currently pursuing the Ph.D. degree with the National Digital Switching System Engineering & Technological Research Center, Henan, China. He joined the School of Computer and Information Engineering, Henan University of Economy and Law, in 2006, as an Associate Professor. His research interests include intelligent information processing, machine learning, and image processing.

JIANHUA PENG was born in 1966. He received the M.S. degree in computer application in 1995. He is currently a Professor and Doctoral Supervisor as well as a Deputy Chief Engineer at the National Digital Switching System Engineering & Technological Research Center, Henan, China. His major research interests include network switching, wireless mobile communication networks, and information secrecy.